

# The evolution of delta-phase in a superplastic Inconel 718 alloy

Yi Huang · Terence G. Langdon

Received: 6 February 2006 / Accepted: 31 May 2006 / Published online: 4 January 2007  
© Springer Science+Business Media, LLC 2007

**Abstract** An Inconel 718 sheet alloy was tested in tension at a temperature of 965°C and an initial strain rate of  $10^{-4} \text{ s}^{-1}$  corresponding to the conditions for optimum superplastic deformation. Detailed observations and quantitative measurements record the evolution of the  $\delta$ -phase during tensile deformation. The experiments show that the total precipitation of the  $\delta$ -phase increases with strain but there is a decrease with strain in the number density of the needle/plate  $\delta$ -phase particles and a corresponding increase with strain in the number density of the blocky/globular  $\delta$ -phase particles.

## Introduction

The Inconel 718 superalloy has a wide range of uses in high-temperature applications including aircraft engines and power generation. Accordingly, much

attention has been devoted to developing and evaluating the superplastic potential of this material [1–7]. The early development of superplastic forming tests and diffusion bonding trials provided a clear demonstration that complex parts may be fabricated from the Inconel 718 alloy using gas–pressure forming [8, 9]. In subsequent detailed evaluations of the superplastic behavior, tests were conducted on samples of the alloy having a grain size less than 6  $\mu\text{m}$  at a temperature of 982°C [1, 2] and later more extensive testing was conducted at 954°C where the strain rate sensitivity was measured as  $\sim 0.4$  at an initial strain rate of  $10^{-4} \text{ s}^{-1}$  [3–7]. To provide a detailed evaluation of superplasticity in this material, extensive testing was conducted using samples of Inconel 718SPF sheet over a range of temperatures from 920 to 1,040°C and with initial strain rates from  $10^{-4}$  to  $10^{-2} \text{ s}^{-1}$  [10]. The results from these tests showed that the maximum value of the strain rate sensitivity was  $\sim 0.37$  and this peak value occurred when the measured elongation was  $\sim 200\%$  at a testing temperature of 965°C using a strain rate of  $10^{-4} \text{ s}^{-1}$ . Accordingly, it was concluded that this corresponds to the condition for optimum forming.

The phases normally present in the Inconel 718 superalloy are discrete MC particles, the needle or plate-like  $\delta$ -phase, the disk-shaped  $\gamma''$ -phase and the spheroid  $\gamma'$ -phase [11]. There have been numerous investigations of the precipitate characteristics and the strengthening mechanisms of the metastable body-centered tetragonal (BCT) coherent precipitate  $\gamma''$  ( $\text{Ni}_3\text{Nb}$ ) phase and the face-centered cubic (FCC) coherent precipitate  $\gamma'$  ( $\text{Ni}_3\text{Al}$ ) phase in Inconel 718 and the influence of these phases on the properties [12–15]. In practice, the major strengthening phase is the  $\gamma''$ -phase and only a small volume fraction ( $<25\%$ ) is

---

Y. Huang  
JVM Castings (Tamworth) Ltd., Borman, Lichfield Road  
Industrial Estate, Tamworth, Staffordshire B79 7TA, UK  
e-mail: yhuang@jvmcastings.com

T. G. Langdon (✉)  
Departments of Aerospace and Mechanical Engineering  
and Materials Science, University of Southern California,  
Los Angeles, CA 90089-1453, USA  
e-mail: langdon@usc.edu

T. G. Langdon  
Materials Research Group, School of Engineering Sciences,  
University of Southampton, Southampton SO17 1BJ, UK  
e-mail: langdon@soton.ac.uk

needed to transform Inconel 718 into a high-strength superalloy. In contrast, the volume fraction of  $\gamma'$ -phase in Inconel 718 is less than 5% and the strengthening contributed by this phase is incidental [16].

The equilibrium structure corresponding to the  $\gamma''$  ( $\text{Ni}_3\text{Nb}$ ) phase is the orthorhombic incoherent  $\delta$  ( $\text{Ni}_3\text{Nb}$ ) phase [17–19]. The precipitation of the  $\delta$ -phase is highly heterogeneous because of the dissimilar structure with respect to the FCC  $\gamma$ -matrix. The precipitation of  $\delta$ -phase occurs in the temperature range of approximately 750–1,020°C. At the lower temperatures, below ~900°C, the precipitation of the  $\delta$ -phase is preceded by  $\gamma''$  precipitation but at higher temperatures the  $\delta$ -phase precipitates directly from the austenite. It has been shown that the most rapid precipitation of the  $\delta$ -phase in Inconel 718 occurs at a temperature of approximately 900°C [20].

It is well established that the equilibrium  $\delta$ -phase has an important influence not only on the microstructure but also on the mechanical properties of Inconel 718. Thus, it has been reported that the  $\delta$ -phase precipitates, whether formed at the grain boundaries or within the matrix, influence the fatigue [21–23], stress-rupture [24–25] and hot working [26–28] properties of the alloy. However, despite the obvious significance of the  $\delta$ -phase, there have been no reports to date concerning the influence of the evolution of the  $\delta$ -phase on the superplastic properties of Inconel 718. The present investigation was initiated to address this deficiency in two ways. First, by evaluating the variations in the presence of the  $\delta$ -phase during superplastic deformation of the alloy. Second, by developing the nature of the relationship between the  $\delta$ -phase, the testing temperature and the strain introduced into the material during tensile testing.

### Experimental material and procedures

An Inconel 718 sheet was provided by Inco Alloys International (Huntington, WV) after cold-rolling to a thickness of 1.6 mm with mill annealing in a continuous annealing furnace for 132 s at 954°C followed by

air-cooling. Table 1 summarizes the chemical composition of the as-received material. Based on the well-established TTT diagram [29], it is anticipated this rapid anneal puts the  $\gamma''$  precipitates into solution so that the matrix is supersaturated with Nb and further exposure to temperatures above 900°C will lead to precipitation and growth of the  $\delta$ -phase. In the as-received condition, the measured average grain size was ~9  $\mu\text{m}$ .

Tensile samples were machined from the as-received sheet and these samples were pulled to failure at a temperature of 965°C using an initial strain rate of  $10^{-4} \text{ s}^{-1}$  in a testing machine operating at a constant rate of cross-head displacement: these conditions were selected because earlier work showed this corresponds essentially to the optimum temperature and strain rate for superplastic deformation of the Inconel 718 alloy [10]. For comparison, a recent report described experiments conducted at 950°C over a range of strain rates using an Inconel 718 alloy obtained from a different source [30]. The tensile tests were interrupted at selected nominal strains in order to evaluate the extent of the development of the  $\delta$ -phase during the deformation process.

Measurements were taken to determine the characteristics of the  $\delta$ -phase precipitation after tensile testing to selected strains. Specifically, quantitative measurements were recorded using a Quantimet 500 image analysis software package and separate measurements were taken of the number density of precipitates, their area fraction and their size. These measurements were undertaken by using a scanning electron microscope, recording ten fields for each strain level at a magnification of 3,500 $\times$  and then further magnifying these micrographs by a factor of approximately 3 $\times$  when transferring to the image analyzing system. It was estimated that the errors associated with the measurements of the sizes of the  $\delta$ -phase was of the order of  $\pm 0.03 \mu\text{m}$ , thereby permitting a reliable estimate of the phase area fraction and the number density. All measurements were carried out on the longitudinal faces of the samples after polishing using diamond paste and then etching for

**Table 1** Chemical composition of as-received Inconel 718 sheet

	Al	B	C	Co	Cr	Cu	Fe	Mn	Mo
wt. %	0.57	0.002	0.02	<0.01	18.11	<0.01	18.40	<0.01	3.03
at. %	1.23	0.01	0.1	<0.01	20.36	<0.01	19.26	<0.01	1.85
	N	Nb	Ni	P	S	Si	Ta	Ti	
wt. %	<0.01	4.95	53.95	0.003	0.0003	0.01	<0.01	0.95	
at. %	<0.042	3.11	53.71	0.006	0.0005	0.02	<0.003	0.27	

5–20 s with Kalling's reagent (4 g  $\text{CuCl}_2$  + 40 ml  $\text{HCl}$  + 60 ml  $\text{C}_2\text{H}_5\text{OH}$ ).

### Experimental results

The occurrence of  $\delta$ -phase precipitation during deformation is illustrated in Fig. 1 where the white particles are the  $\delta$ -phase, the photomicrograph labeled (a) is for the untested condition at zero strain and the other photomicrographs are for nominal strains of (b) 0.16, (c) 0.35, (d) 0.55 and (e) 1.0, respectively. At zero strain it is apparent that the  $\delta$ -phase precipitates occur in a banded structure and there are areas within the matrix where the density of precipitates is very low. Similar bands were visible in the initial stages of deformation although the extent of the non-uniformity gradually decreased with

increasing strain: examples are shown in Fig. 1b at a strain of 0.16 and Fig. 1c at a strain of 0.35. At even higher strains, the distribution of the  $\delta$ -phase became more uniform, as is evident from inspection of Fig. 1d and e at strains of 0.55 and 1.0, respectively. Thus, the  $\delta$ -phase is initially distributed non-uniformly during the tensile deformation but the precipitation becomes more uniformly distributed as the strain increases.

The appearance of the precipitates is shown at a higher magnification in Fig. 2 for strains of (a) 0.16, (b) 0.35, (c) 0.55 and (d) 1.0, respectively. It is apparent that the  $\delta$ -phase precipitates both within the grains in a lamellar form (needle or plate) and at the grain boundaries where it has a more equiaxed and blocky or globular appearance. In general, the precipitates become more blocky or globular and less needle-like or plate-like as the level of deformation increases.

**Fig. 1** The  $\delta$ -phase distribution following deformation at  $965^\circ\text{C}$  with a strain rate of  $10^{-4} \text{ s}^{-1}$  to  $\varepsilon = 0$  (a),  $\varepsilon = 0.16$  (b),  $\varepsilon = 0.35$  (c),  $\varepsilon = 0.55$  (d) and  $\varepsilon = 1.0$  (e)

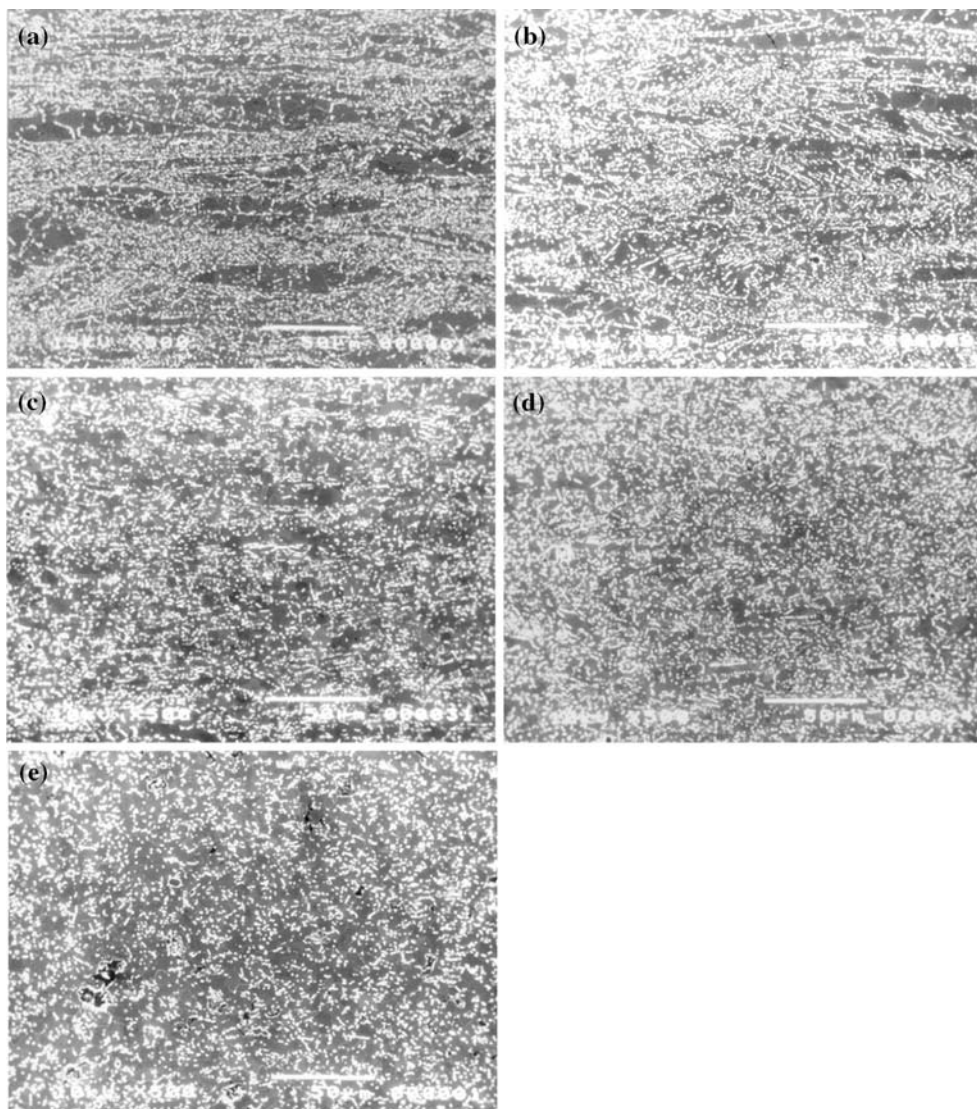
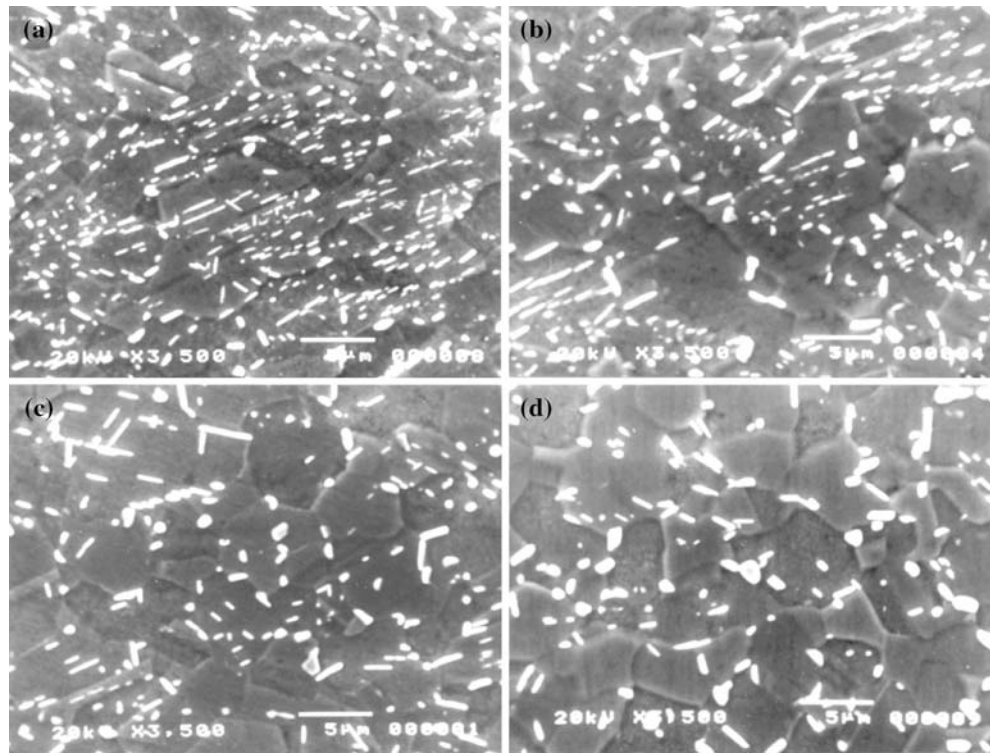


**Fig. 2** The  $\delta$ -phase morphology at 965°C with a strain rate of  $10^{-4} \text{ s}^{-1}$  at  $\varepsilon = 0.16$  (a),  $\varepsilon = 0.35$  (b),  $\varepsilon = 0.55$  (c) and  $\varepsilon = 1.0$  (d)

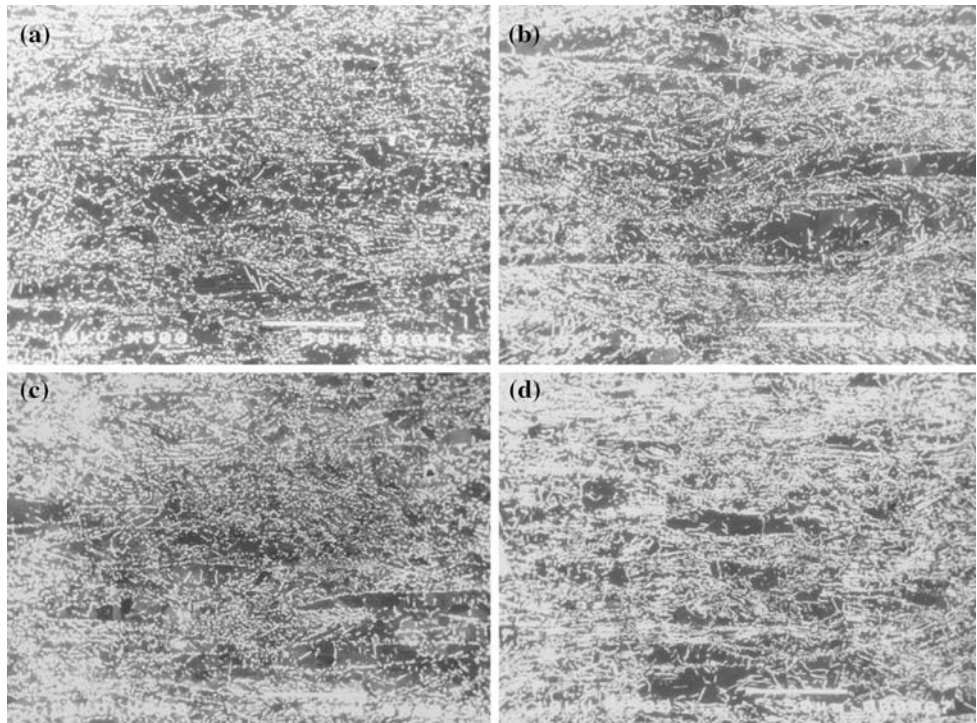


For comparison purposes, Fig. 3 shows photomicrographs recorded in the undeformed material after holding at a temperature of 965°C for periods of (a) 33 min, (b) 65 min, (c) 98 min and (d) 170 min. In the undeformed matrix, and in contrast to the deformed

material, it is apparent that the  $\delta$ -phase precipitates remain non-uniformly distributed.

The distributions of the sizes of the  $\delta$ -phase are shown in Fig. 4 following deformation to selected strains up to a maximum of 1.0. It is apparent that at

**Fig. 3** The  $\delta$ -phase evolution in the undeformed material at 965°C after 33 min (a), 65 min (b), 98 min (c) and 170 min (d)



zero strain, shown on the right, the relative frequency exhibits a single peak with a small tail and the maximum relative frequency of ~60% relates to the  $\delta$ -phase having a thickness of 0.1–0.2  $\mu\text{m}$ . However, as the strain increases to 1.0 the relative frequency gradually transforms to two peaks with a long tail. Thus, at a strain of 1.0 the maximum relative frequency of ~30% corresponds to a thickness of 0.1–0.2  $\mu\text{m}$  but there is also a second peak with a relative frequency of ~13% corresponding to a  $\delta$ -phase thickness of 0.4–0.5  $\mu\text{m}$ . Thus, the distribution of the thicknesses of the  $\delta$ -phase changes from a narrow range at the lower strains to a relatively wide range at the higher strain.

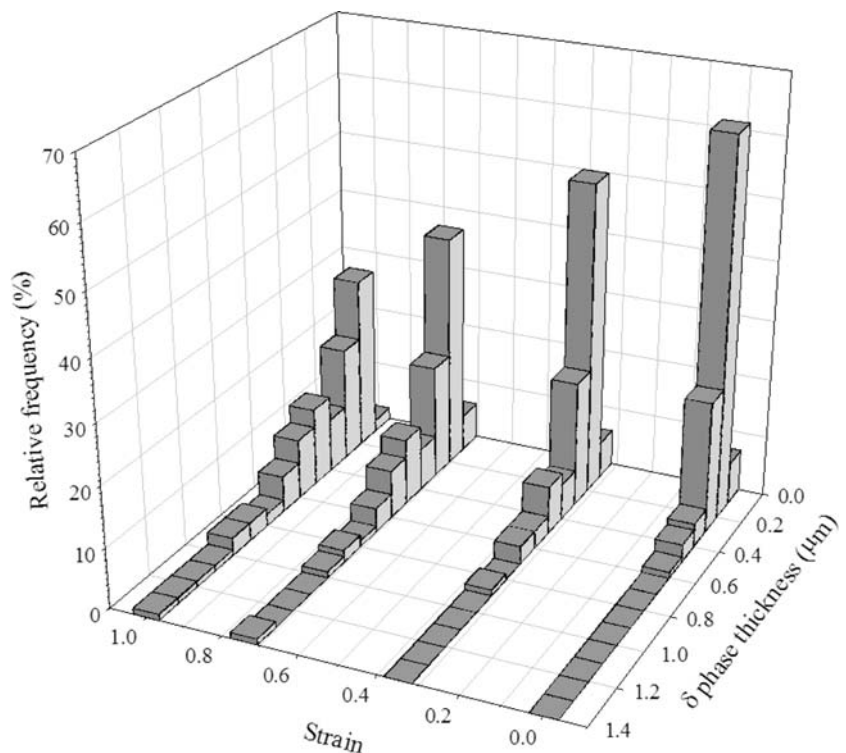
For statistical analysis, the morphology of the  $\delta$ -phase was divided according to the  $\delta$ -phase particle thickness. Thus, if the thickness was greater than 0.35  $\mu\text{m}$  the  $\delta$ -phase was considered to belong to the blocky or globular category whereas if the thickness was less than 0.35  $\mu\text{m}$  the  $\delta$ -phase was considered to belong to the needle or plate category. Quantitative analyses of the  $\delta$ -phase area fraction (as a percentage) and the  $\delta$ -phase density (as  $\mu\text{m}^{-2}$ ) are shown in Figs. 5 and 6 where the area fraction of 2.64% for the total amount of the  $\delta$ -phase present in the alloy at zero strain corresponds to the measured area fraction after heating to 965°C and holding at temperature for 20 min prior to tensile testing. It follows from inspection of Fig. 5 that the total extent of the  $\delta$ -phase

increases with increasing strain but there is a corresponding reduction in the extent of the needle or plate-like precipitates, and from Fig. 6 it is concluded that the density of the  $\delta$ -phase decreases significantly from 0.36 to 0.14  $\mu\text{m}^{-2}$  with increasing strain but there is a concomitant small increase in the density of the blocky or globular precipitates over the same strain increment.

## Discussion

Very little information is available on the influence of composition on  $\delta$ -phase formation in the Inconel 718 alloy. The saturation level of the  $\delta$ -phase precipitate, corresponding to the equilibrium content, depends on the temperature and the specific composition of the alloy. Thus, Liu et al. [31] reported an equilibrium content of the  $\delta$ -phase of about 5.7 wt.% (equivalent to 10.3 vol.%) at 965°C when using an alloy with composition (in wt.%) of 5.10% Nb, 0.11% Si, 0.50% Al, 1.0% Ti, 1.50% (Al + Ti) and an Al/Ti ratio of 0.5. Comparing this composition with the composition for the present alloy listed in Table 1, it appears that the as-received Inconel 718 sheet is slightly low on Nb and Si, slightly high on Al, the Al/Ti ratio is high and the (Al + Ti) concentration is almost identical. There is experimental evidence showing that high concentrations of Nb and Si and a low value of Al promote

**Fig. 4** The  $\delta$ -phase size distribution at 965°C with a strain rate of  $10^{-4} \text{ s}^{-1}$



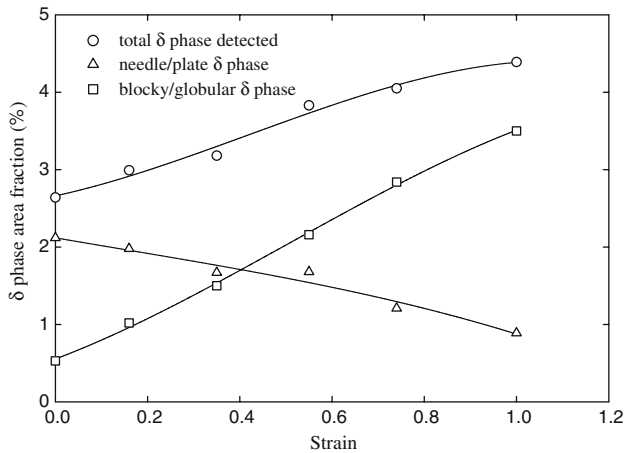


**Fig. 5** The  $\delta$ -phase precipitation area fraction versus strain

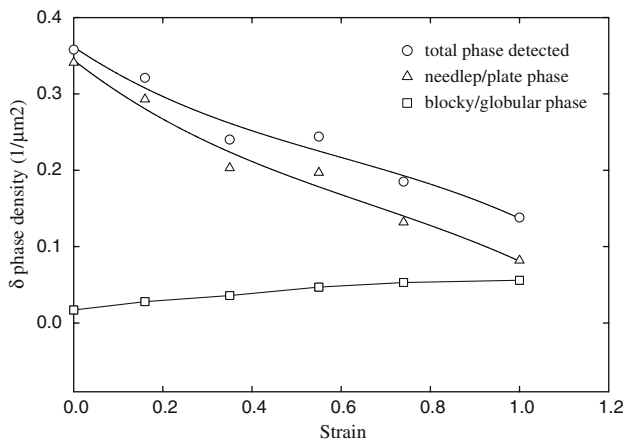


**Fig. 6** The  $\delta$ -phase precipitation density versus strain

$\delta$ -phase precipitation [32]. On the other hand, Collier et al. [19] showed that the driving force to form the  $\delta$ -phase in a nickel-based alloy decreased with increasing Al/Ti ratio and (Al + Ti) concentration. Accordingly, the equilibrium content of the  $\delta$ -phase at 965°C in the present Inconel 718 sheet, although not known exactly, should be lower than the equilibrium content of 5.7 wt.% (equivalent to 10.3 vol.%) reported by Liu et al. [31]. This is consistent with the observation that, after heating for 20 min at 965°C before tensile testing and at zero strain, the  $\delta$ -phase area fraction was only 2.64% which is lower than the reported equilibrium concentration of 5.7 wt.% or 10.3 vol.%. Considering the relatively low  $\delta$ -phase content of 2.64% at zero strain, and by comparison with the reported equilibrium concentration of 10.3 vol.%, it is reasonable to assume that this value is far below the equilibrium content for the present alloy. This is consistent with the experimental results in Fig. 5 where the  $\delta$ -phase area fraction increases with increasing strain.

Based on the microstructures in Fig. 1, the starting material has banded  $\delta$ -phase precipitates due to residual segregation within the sheet. As deformation continues, these banded regions gradually disappear. In the undeformed specimens, as shown in Fig. 3, the banded  $\delta$ -phase is continually present. Thus, these results provide a clear comparison of the variations of the banded  $\delta$ -phase precipitates between the deformed and undeformed areas and they indicate that deformation affects both the disappearance of the banded  $\delta$ -phase regions and the corresponding change in morphology of the  $\delta$ -phase.

The factors controlling the morphology of the  $\delta$ -phase are complex. It is known that the plate-like  $\delta$ -phase precipitates in the  $\gamma$  matrix mainly along  $(111)_\gamma$  in an intragranular form while the globular  $\delta$ -phase precipitates primarily on the grain boundaries [33]. Desvallees et al. [27] found that the stable morphology of the  $\delta$ -phase depended mainly on the temperature such that for heat treatments below 930°C the stable morphology was plate-like whereas spherical  $\delta$ -phase precipitates were formed as the temperature increased. For the Inconel 718 sheet used in the present experiments, the temperature remained constant at 965°C during the deformation process and it is therefore concluded the deformation process and the time contribute to the dissolution of the needle-like and plate-like  $\delta$ -phase and the concomitant growth of the blocky and globular  $\delta$ -phase. These general trends are visible in Fig. 6 and it is evident from Fig. 4, and supported by the pictorial evidence in Fig. 2, that the  $\delta$ -phase precipitation thickness increases with strain.

There are two possible explanations for the increase in the blocky/globular  $\delta$ -phase and the corresponding decrease in the needle/plate  $\delta$ -phase with increasing strain. The first possibility is that the needle/plate  $\delta$ -phase has a larger surface energy than the blocky/globular  $\delta$ -phase so that the needle-like and plate-like precipitates are less energetically stable. This suggests a tendency for the needle/plate  $\delta$ -phase to dissolve during the deformation process and to grow into a more blocky morphology in order to attain a lower surface energy. The second possibility is related to the migration of a high-angle boundary through the  $\delta$  precipitates which may lead to a dissolution of most of the needle/plate  $\delta$ -phase, the loss of their orientation relationship with the matrix for any small amount of remaining needle/plate  $\delta$ -phase, followed by the growth of this remaining phase into a blocky  $\delta$ -phase. There is some support for the latter proposal because an essentially similar trend was reported by Nes [34] when investigating the hot deformation of an Al–Cu–Zr (Supral) alloy. In the work on the Al–Cu–Zr alloy,

it was found that a migrating boundary was capable of dissolving all of the smaller particles thereby leaving behind a distribution of coarser incoherent dispersoids. In view of the latter experimental observation, it is reasonable to conclude that boundary migration and particle dissolution may play at least a partial role in the evolution of the  $\delta$ -phase during deformation of the Inconel 718 alloy.

### Summary and conclusions

1. Experiments were conducted on the Inconel 718 alloy to evaluate the evolution of the  $\delta$ -phase during deformation at a temperature of 965°C and strain rate of  $10^{-4} \text{ s}^{-1}$  corresponding to the conditions for optimum superplastic deformation.
2. The results show that the total precipitation of the  $\delta$ -phase increases with strain, the number density of the needle/plate  $\delta$ -phase particles decreases with strain and the number density of blocky/globular  $\delta$ -phase particles increases with strain under these testing conditions.

**Acknowledgements** One of the authors (Y. Huang) acknowledges the financial support of the School of Metallurgy and Materials of the University of Birmingham and the Committee of Vice-Chancellors and Principals (CVCP) of the Universities of the United Kingdom for an ORS award. The authors also acknowledge the contributions to this project from Dr. P. L. Blackwell and Dr. M. Strangwood.

### References

1. Mahoney MW, Crooks R (1988) In: Heikkinen HC, McNelley TR (eds) Superplasticity in aerospace. The Metallurgical Society, Warrendale, PA, p 331
2. Mahoney MW (1989) In: Loria EA (eds) Superalloys 718—metallurgical and applications. The Minerals, Metals & Materials Society, Warrendale, PA, p 391
3. Smith GD, Yates DH, Comley PN, Ma Y, Langdon TG (1992) In: Antolovich SD, Stusrud RW, MacKay RA, Anton DL, Khan T, Kissinger RD, Klarstrom DL (eds) Superalloys 1992. The Minerals, Metals & Materials Society, Warrendale, PA, p 43
4. Smith GD, Yates DH, Daniel H (1994) In: Loria EA (ed) Superalloys 718, 625, 706, and various derivatives. The Minerals, Metals & Materials Society, Warrendale, PA, p 355
5. Smith GD, Flower HL (1995) In: Ghosh AK, Bieler TR (eds) Superplasticity and superplastic forming. The Minerals, Metals & Materials Society, Warrendale, PA, p 117
6. Smith GD, Flower HL, Leholm RB (1996) In: Haggatt JT, Falcone A, Nelson KM, Hill SG (eds) Technology transfer in a global community. Society for the Advancement of Material and Process Engineering, Covina, p 611
7. Smith GD, Gregory SR, Ma Y, Li Y, Langdon TG (1997) In: Loria EA (ed) Superalloys 718, 625, 706 and various derivatives. The Minerals, Metals and Materials Society, Warrendale, PA, p 303
8. Chandler WT, Ghosh AK, Mahoney WM (1984) J Spacecr 21:61
9. Yeh MS, Tsau CW, Chuang TH (1996) J Mater Eng Perform 5:71
10. Huang Y, Strangwood M, Blackwell PL (2000) Mater Sci Tech 16:1309
11. Loria EA (1988) J Metals 40(7):36
12. Cozar R, Pineau A (1973) Met Trans 4:47
13. Sundaraman M, Mukhopadhyay P, Banerjee S (1988) Acta Met 36:847
14. Sundaraman M, Mukhopadhyay P, Banerjee S (1992) Met Trans A 23:2015
15. Slama C, Servant C, Cizeron G (1997) J Mater Res 12:2298
16. Yang L, Chang KM, Mannan S, deBarbadillo J (1997) In: Loria EA (eds) Superalloys 718, 625, 706 and various derivatives. The Minerals, Metals and Materials Society, Warrendale, PA, p 353
17. Boesch WJ, Canada HB (1969) J Metals 21(10):34
18. Sundaraman M, Mukhopadhyay P, Banerjee S (1988) Met Trans A 19:453
19. Collier JP, Wong SH, Phillips JC, Tien JK (1988) Met Trans A 19:1657
20. Moll JJ, Maniar GN, Muzyka DR (1971) Met Trans 2:2143
21. Hong BD, Yi X, Meng QC (1991) Acta Met Sinica 27:A55
22. Li SQ, Zhuang JY, Yang JY, Deng Q, Du JH (1994) In: Loria EA (eds) Superalloys 718, 625, 706 and various derivatives. The Minerals, Metals and Materials Society, Warrendale, PA, p 545
23. Zhang Y, Huang XB, Wang Y, Yu WC, Hu ZQ (1997) In: Loria EA (ed) Superalloys 718, 625, 706 and various derivatives. The Minerals, Metals and Materials Society, Warrendale, PA, p 229
24. Muzyka DR, Maniar GN (1969) ASM Metals Eng Q 9:23
25. Moll JJ, Maniar GN, Muzyka DR (1971) Met Trans 2:2153
26. Radavich JF, Coutts WH Jr (1984) In: Gell M, Kortovich CS, Bricknell RH, Kent WB, Radavich JF (eds) Superalloys 1984. The Minerals, Metals and Materials Society, Warrendale, PA, p 497
27. Desvallees Y, Bouzidi M, Bois F, Beaud N (1994) In: Loria EA (eds) Superalloys 718, 625, 706 and various derivatives. The Minerals, Metals and Materials Society, Warrendale, PA, p 281
28. Srinivasan N, Prasad YVRK (1994) Metl Mater Trans A 25:2275
29. Garcia CL, Lis AK, Loria EA, Deardo AJ (1992) In: Antolovich SD, Stusrud RW, MacKay RA, Anton DL, Khan T, Kissinger RD, Klarstrom DL (eds) Superalloys 1992. The Minerals, Metals and Materials Society, Warrendale, PA, p 527
30. Huang Y, Langdon TG (2005) Mater Sci Eng A 410–411:130
31. Liu WC, Chen ZL, Yao M (1999) Met Mater Trans A 30:31
32. Brown EE, Muzyka DR (1987) In: Sims CT, Stoloff NS, Hagel WC (eds) Superalloys II. Wiley, New York, p 65
33. Kirman I, Warrington DH (1970) Met Trans 1:2667
34. Nes E (1979) Metal Sci 13:211